International Journal of Fluid Machinery and Systems
Vol. 4, No. 3, July-September 2011

DOI: 10.5293/IJFMS.2011.4.3.341
ISSN (Online): 1882-9554

Original Paper

Computational Fluid Dynamics Modeling Studies on Bacterial Flagellar Motion

Manickam Siva Kumar[1] and Pichai Philominathan[2]

[1]Department of Physics, Indian School Muscat, the Sultanate of Oman
shiva@eeclubs.org
[2]Department of Physics, AVVM SriPushpam College, Tanjore, India
philominathan@gmail.com

Abstract

The study of bacterial flagellar swimming motion remains an interesting and challenging research subject in the fields of hydrodynamics and bio-locomotion. This swimming motion is characterized by very low Reynolds numbers, which is unique and time reversible. In particular, the effect of rotation of helical flagella of bacterium on swimming motion requires detailed multi-disciplinary analysis. Clear understanding of such swimming motion will not only be beneficial for biologists but also to engineers interested in developing nanorobots mimicking bacterial swimming. In this paper, computational fluid dynamics (CFD) simulation of a three dimensional single flagellated bacteria has been developed and the fluid flow around the flagellum is investigated. CFD-based modeling studies were conducted to find the variables that affect the forward thrust experienced by the swimming bacterium. It is found that the propulsive force increases with increase in rotational velocity of flagellum and viscosity of surrounding fluid. It is also deduced from the study that the forward force depends on the geometry of helical flagella (directly proportional to square of the helical radius and inversely proportional to pitch).

Keywords: Flagellar hydrodynamics, helical swimming motion, low Reynolds number and computational fluid dynamics.

1. Introduction

The Computational Fluid Dynamics (CFD) has been used in various areas of biology and sports science to investigate swimming mechanisms. A detailed analysis using CFD methods enabled us to understand the drag and propulsion generated during swimming of dolphin [1]. The use of CFD in nano-scale domain is also becoming increasingly popular. Miniature or nano-scale swimming robots are beneficial for screening and treatment of many diseases. They are biologically inspired and designed based on bacterial motion. Studying bacterial swimming motion using experiments involves lots of practical difficulties, CFD methodologies –which offer alternative ways to experiments, will help us to understand fluid dynamics of swimming motion.

Many prokaryotic bacteria like Escherichia Coli during chemotaxis, swim towards or away from certain chemicals using their flagella [2]. It has been proved experimentally that it is flagellar rotation that causes swimming motion [3]. Each flagellum extends from the cell body and is rotated by reversible flagellar motor situated at the base. The rotational speed of the motor ranges from 15 – 300 Hz during swimming and the swimming speed of the bacteria is 10-35μm/s. Flagellum grows like an appendage up to 10-15 μm in length and through its atomic structure study, it has been proved that there are 11 protofilaments (protein monomers) whose structural change causes change in flagellar handedness, amplitude and pitch [4].

The hydrodynamic force produced is characterized by fluid's viscosity; low Reynolds number flow and diffusion (see our recent review on the physics of flagellar motion for more details [5]).

There are two modes of motion available during swimming they are 'run' and 'tumble'. During run mode flagellar motor rotates clockwise (as viewed from outside the cell) and the left-handed helical filaments bundle together. As flagellum is left-handed helical, clockwise rotation produces a force on the cell body. During tumble, due to a complex process, left-handed helix is transformed into right-handed helix. The tumble is due to flagellar counter- clockwise rotation and pauses. In this paper we analyze the flow and model the 'run' mode of bacterial motion using commercial CFD software SolidWorks © 2010 Flow Simulation.

Received June 7 2011; accepted for publication June 15 2011; Review conducted by Dr. Shogo Nakamura. (Paper number O11012J)
Corresponding author: Pichai Philominathan, Professor, philominathan@gmail.com

2. Mathematical modeling of low Reynolds number flow

The Reynolds number is defined as the ratio of inertial force and viscous force. In the case of helix of pitch λ rotating with the speed ω, in fluid with dynamic viscosity μ , the Reynold's number is given by [6]

$$\mathrm{R_e} = \frac{\omega \lambda^2 \rho}{\mu} \tag{1}$$

If we substitute the typical values for *E. coli*, we will get Re = 10^{-05}. This very low value indicates that swimming motion of this type has no inertia, no coasting and time-reversible thus unique.

In such a case of low Reynolds number domain, the flow is often called Stokes or creeping flow. The stokes equation and equation of continuity becomes

$$\mu \nabla^2 u - \nabla p = 0 \tag{2}$$

$$\nabla u = 0 \tag{3}$$

Note that the eqn. (3) is due to restrictive conditions of continuity. In order to solve these equation visualize flow fields and modeling with various configurations, we have used SolidWorks 2010 Flow Simulation – a commercial CFD software which has built in 3D modeling module for preprocessing and flow simulation add-in with capabilities of post processing.

3. The Flow Simulation CFD methodology

The incompressible, unsteady Navier-Stokes equations are given by

$$\begin{aligned}
\frac{\partial u}{\partial t} + u\frac{\partial u}{\partial x} + v\frac{\partial u}{\partial y} + w\frac{\partial u}{\partial z} &= -\frac{1}{\rho}\frac{\partial p}{\partial x} + \nu\left(\frac{\partial^2 u}{\partial x^2} + \frac{\partial^2 u}{\partial y^2} + \frac{\partial^2 u}{\partial z^2}\right) \\
\frac{\partial v}{\partial t} + u\frac{\partial u}{\partial x} + v\frac{\partial u}{\partial y} + w\frac{\partial u}{\partial z} &= -\frac{1}{\rho}\frac{\partial p}{\partial y} + \nu\left(\frac{\partial^2 v}{\partial x^2} + \frac{\partial^2 v}{\partial y^2} + \frac{\partial^2 v}{\partial z^2}\right) \\
\frac{\partial w}{\partial t} + u\frac{\partial u}{\partial x} + v\frac{\partial u}{\partial y} + w\frac{\partial u}{\partial z} &= -\frac{1}{\rho}\frac{\partial p}{\partial z} + \nu\left(\frac{\partial^2 w}{\partial x^2} + \frac{\partial^2 w}{\partial y^2} + \frac{\partial^2 w}{\partial z^2}\right)
\end{aligned} \tag{4}$$

with the equation of continuity,

$$\frac{\partial u}{\partial x} + \frac{\partial v}{\partial y} + \frac{\partial w}{\partial z} = 0 \tag{5}$$

where x, y and z are the axes of the orthogonal coordinate system. *u*, *v* and *w* are the fluid velocity vectors in each direction respectively. *p* is the pressure and *ρ* is the fluid density. These equations are to be solved in a given computational domain in each mesh cell [7].

3.1 Rotating regions

The local rotating regions is an option employed for calculating transient or steady state flows in regions around rotating solid parts. This rotating region has its own rotating coordinate system. The Navier-Stokes equation is solved in stationary regions of the computational domain in the inertial Cartesian coordinate system. The influence of the rotational effect on the flow is taken into account in the equations written in each of the rotating coordinates.

The solution obtained within the rotating regions and non-rotating regions of the computational domain are connected using special internal boundary conditions at the fluid boundaries of the rotating regions. This is done by slicing the rotating regions into rings of equal width. The values of flow parameters are taken as boundary conditions from the neighboring regions and averaged circumferentially over each of these rings. An iterative procedure is used to solve the problem by adjusting the solutions in the rotating and non-rotating regions with the relaxations.

3.2 Computational mesh

The flow simulation uses a rectangular computational domain. This is automatically constructed so that it encloses the solid body and associated boundary planes. The flow simulation consists of three steps in mesh building. First is a basic mesh building in which the computational domain is sliced by the basic mesh planes. This is independent of solid-fluid interface. The second step is to splitting cells along the solid-fluid interface. These child cells are then refined according to the solid-fluid curvature. As a result of such meshing procedures, a locally refined computational mesh is obtained and used for solving the conservation equations on it.

3.3 Numerical solutions technique

The Flow Simulation uses finite volume (FV) approach to solve the governing equations. This involves a rectangular computational mesh designed in Cartesian coordinate system with the locally refinement of the mesh at the solid-fluid interface. The values of the physical variables are stored at the centers of the mesh cell. The governing equations are discretized, the spatial derivatives are approximated with implicit second-order accuracy and the time derivatives are approximated with an implicit first-order Euler scheme. Flow Simulation uses double-preconditioned iterative procedure based on multigrid method to solve equations [8].

4. Methods and materials

4.1 Three dimensional model

The aim of CFD analysis is to visualize the flow field generated by the helical flagella and to conduct model studies to investigate the factors affecting the swimming motion. A typical bacterium like *E. coli* consists of a cell body and flagellum. During 'run' modes, the flagellum becomes rigid helix.

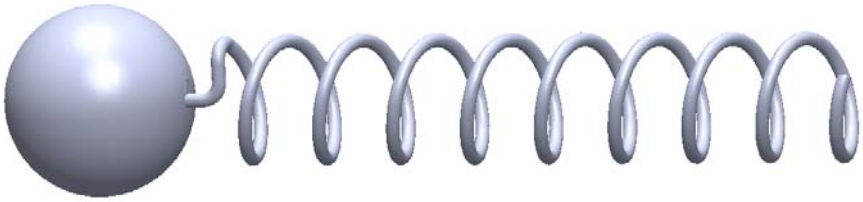

Fig. 1 the helical flagellum with a cell body

The flagellar filament is modeled as a helix with solid tube of thickness 2r and of helical radius 'R', pitch 'λ' and length 'L'. Helices with various configurations were also built for modeling studies. All helices were having short pitch angles, i.e. $\theta \approx 2\pi R / \lambda$ was very small.

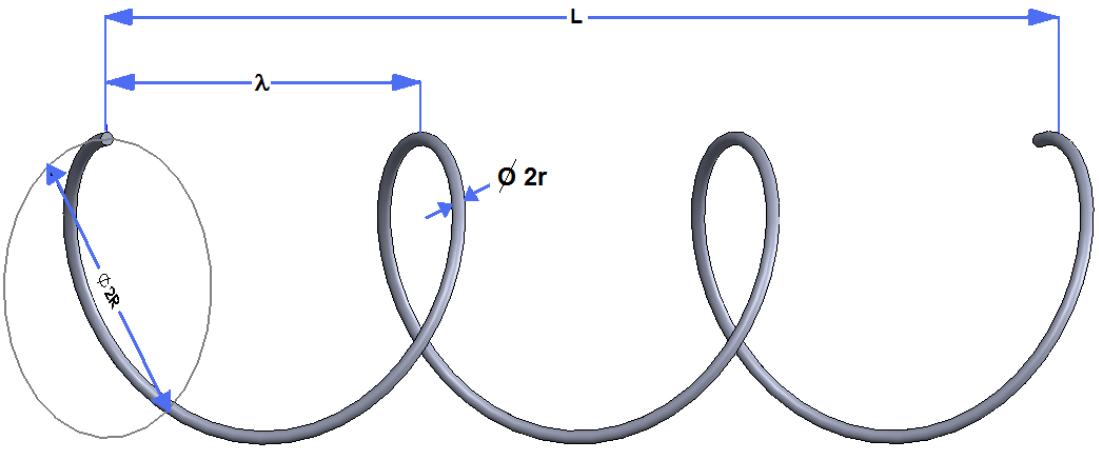

Fig. 2 The flagellum. Modeled as helical tube with radius r = 1mm with configurations, R= 12.7, 17.7, 22.7 and 27.7mm. Pitch length with λ = 66, 76, 86, 96 and 106 mm.

Though the **Fig. 2** dimensions of the models were chosen in macro-scale for better visualization of flows, fluid viscosity and density are kept high such that the Reynolds number becomes ≈ 10^{-05}.

4.2 Meshing

Based on the geometry and boundaries of the model, computational domain was automatically created by Flow Simulation. The mesh is created using 'solid-fluid interface curvature' constraint. Due to this a locally refined meshing can be seen along the walls of flagellum (inset of Figure 3). Table 1 shows the number of cells in mesh for the configuration R=22.7 mm and λ =66mm.

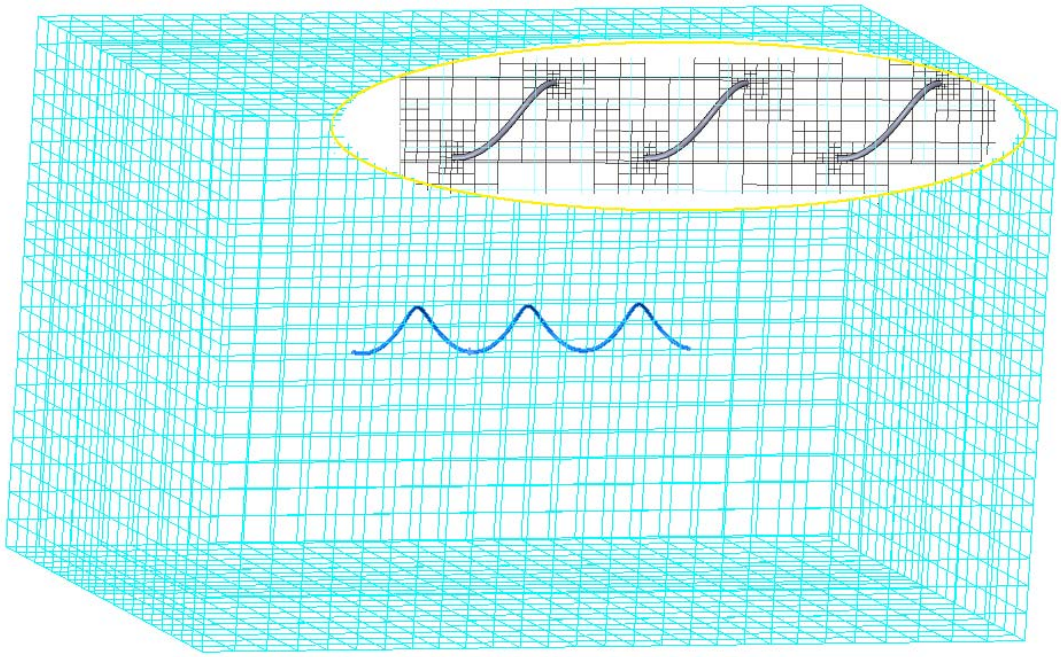

Fig. 3 Three dimensional model of helix in computational mesh. Inset: cross-section of finer refined mesh along the helix

Table 1 Number of cells in mesh

Parameter	Value
Total cells	24746
Fluid cells	15426
Solid cells	413
Partial cells	8907
Irregular cells	0
Trimmed cells	76

4.3 Prescribed rotational motion and measurement of goals

A cylindrical fluid volume around flagella is chosen as rotating region. And a rotational velocity was prescribed along Y-axis. The coupled motion produced due to this rotation was observed in the CFD studies.

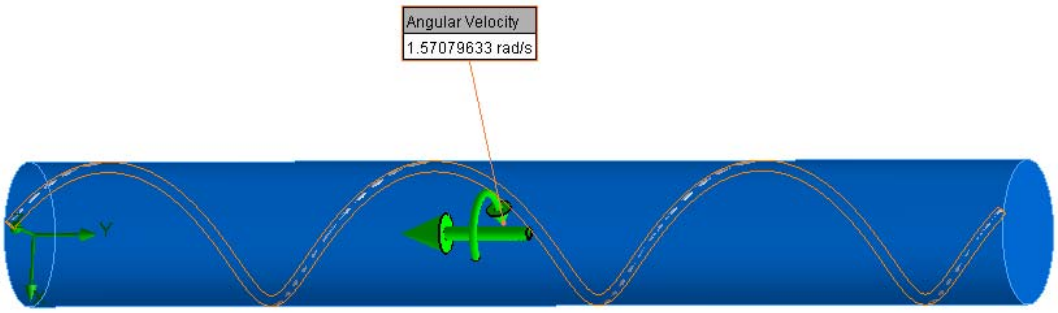

Fig. 4 Local rotating fluid region around helix

Flow simulation has a built in option to measure various physical quantities during the study. They can be obtained through setting ‘goals’ during preprocessing. They include global, volume, surface or point goal associated with the selected parts. Mainly forward thrust force (experienced by the helical surface), velocity (produced on fluid volume enclosed) and pressure were measured.

5. Results and Discussion

Many theories, including slender body theory and resistive-force theory suggest that the parameters that influence swimming include: rotational speed of flagella, viscosity of the fluid and helical geometry [5]. The CFD studies were conducted by varying one of these parameters by keeping rest of them constant.

The flow pattern for the configuration helical radius 22.7 mm and rotational velocity 1.57 rad/s, with fluid viscosity 100 Pa S is obtained. Contour graphs depicting velocity and pressure in XY plane is seen through a cut plot. The visualization of flow fields and contours show a forward movement as expected in the case of low Reynolds number domain. The effect of rotational motion of the helix is seen and high pressure zones are visible at the rear sides of the flagellum

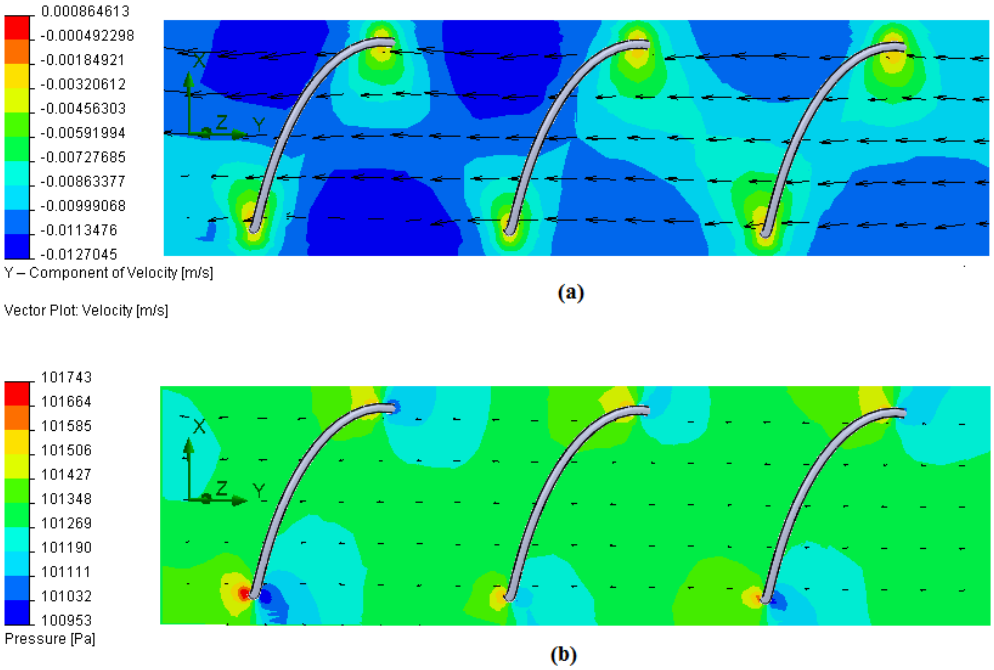

Fig. 5 Contour plots of velocity and pressure for the configuration helical radius 22.7 mm and rotational velocity 1.57 rad/s
(a) velocity vector plot shows the fact that there is a coupled translational motion along Y-axis.
(b) Pressure plot shows the pressure drops at rear side of the helix shows translational motion of the flagellum along +Y-axis.

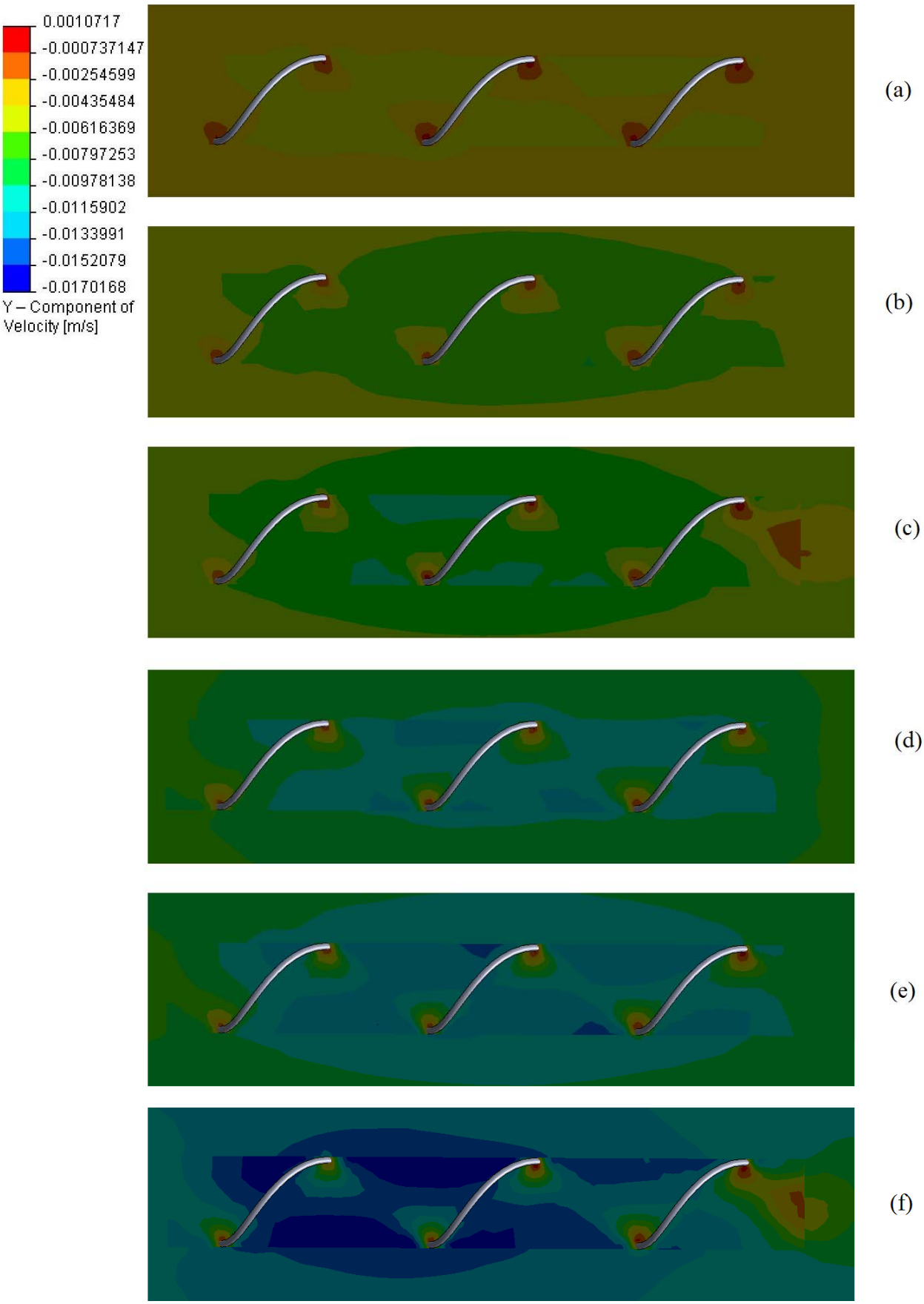

Fig. 6 Y-Component velocity at various rotational speeds. The helical flagella is rotated with configuration R= 12.7 mm and λ = 66 mm is rotated at the speeds (a) 1.57 rad/s; (b) 2.20rad/s ; (c) 2.83 rad/s; (d) 3.46 rad/s; (e) 4.08rad/s; and (f) 4.71rad/s. The Y-component velocity is high after the flow is developed and in –Y direction.

The velocity contour plot clearly indicates the effect of rotational speed in axial motion. On increasing rotational speed, the forward velocity of the flagellum increases. The axial thrust in each case also was measured through surface goal option and shows a linear relation as expected (Figure 7 b).

The next study has been conducted by varying only helical radius. At a constant rotational speed of 1.57 rad/s, the helical radius was changed to 12.7, 17.7, 22.7 and 27.7 mm. The propulsive force was measured in each case. It is found that the force is directly proportional to the square of the radius of the helical filament (Figure 7 a). Simulations were also continued for various rotational speeds of helical flagella. This time helical radius was fixed constant at 25.4 mm and 35.4 mm. This study illustrated that on increasing the rotational velocity, the propulsive force also increases. The slope of this graph shows the value of coupling coefficient transforming rotational velocity with the propulsive force produced (Figure 7 b).

The next study involved the simulations with various values of pitch of the helix 77, 88, 99, 110, 121 mm. The rotational speed was fixed at 1.57rad/s and radius of helix used was 12.7 mm. It was found from the data that, on increasing the pitch of the helix, the propulsive force is decreasing (Figure 7 c). In order to understand the effect of viscosity in the propulsive force, at a pitch of 66 mm and rotational speed of 1.57 rad/s, viscocity is varied between 100 to 125 with the units of 5. The result indicates that on increasing the viscosity the axial force increases linearly (Figure 7d).

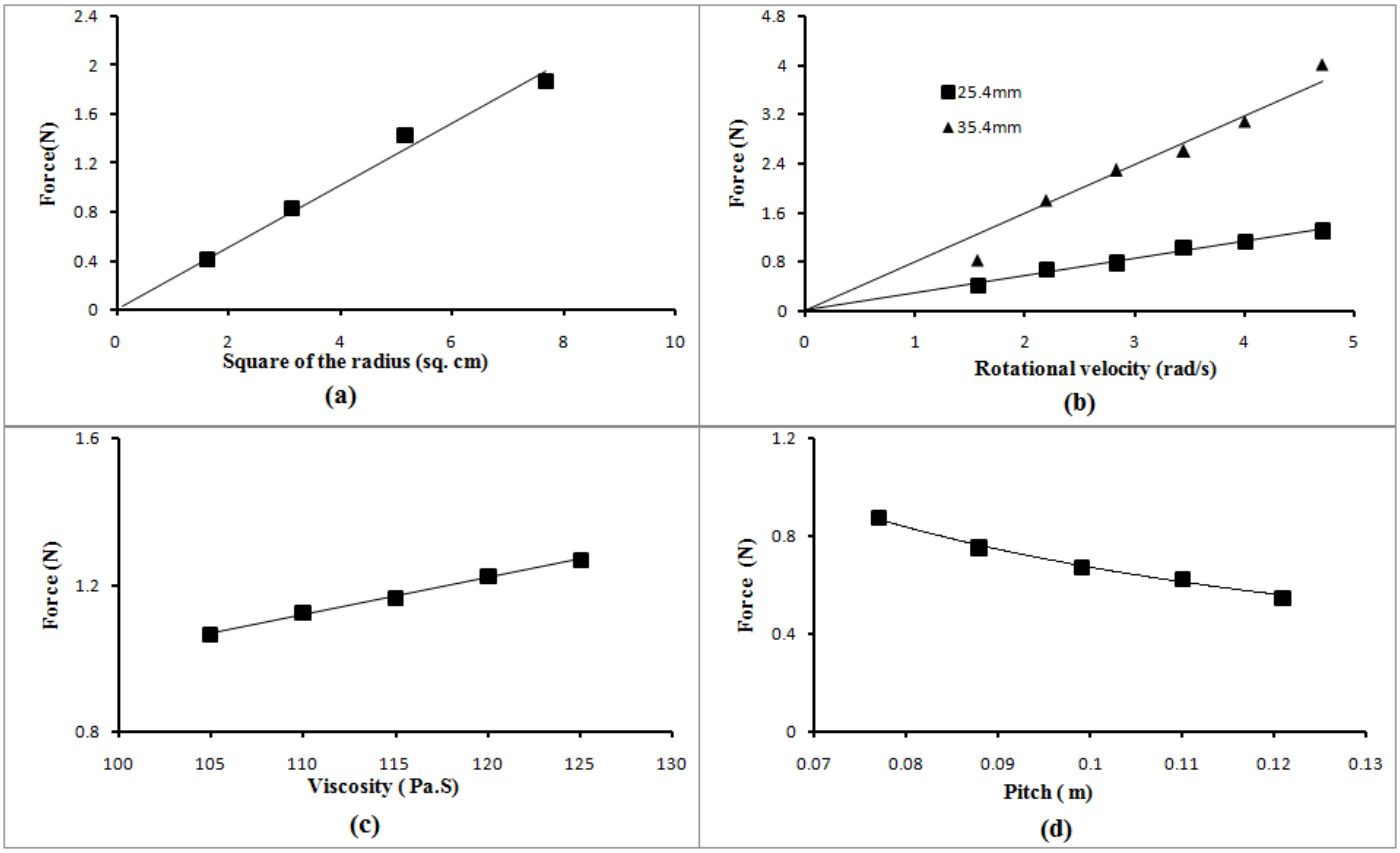

Fig. 7 Results of the studies to investigate the dependencies of propulsive force.

(a). Influence of the helical radius on axial thrust. Graph between propulsive force and the square of the radius which indicates the fact that $F \propto R^2$.

(b). Effect of rotational speed and helical radius on propulsive force.

(c) Influence of helical pitch on propulsive force showing inverse proportion. This fact biologically signify that bacteria with shortly pitched flagella can be effective during chemotaxis.

(d) Influence of viscosity of surrounding fluid on propulsive force. Unlike the high Reynolds number domain, increasing viscosity increases propulsive force.

5.1 Validation

In order to validate these CFD studies, we can use Buckingham-π theorem. This theorem applies dimensional analysis to compare model to a prototype. According to this theorem, the ratio of $F / \mu\omega L^2$ should be same for simulated one and real one [9]. Taking the typical values of a bacterium (*E. coli*) the values of length, viscosity and rotational velocity are 10μm, 0.001 Pa.S, 314 rad/s respectively. Taking the case of simulation where L= 20cm, η =100 Pa.S, ω = 1.57 rad/s, the propulsive force computed was F =0.4172N. The actual force is calculated using Buckingham-π theorem found to be in the range of 10^{-12} N which is in agreement with the reported propulsive force measurements due to single helical flagella using direct experiment methods [10].

6. Conclusions & Future work

It is difficult to conduct experiments in the laboratory with the parameters of the helical flagellum changed. These CFD modeling studies enabled us to vary the dependencies and measure the parameters with the help of Flow Simulation software.

The results of the simulation, which is in accordance with the experimental results, illustrated the following facts:

i) On increasing the rotational speed, the axial thrust developed increases.

ii) The axial thrust is also found to be directly proportional to the square of the radius of the helix.

iii) On increasing the pitch of the helix, the axial force developed decreases.

iv) The helical thrust developed increases on increasing the viscosity of the surrounding fluid.

By taking these findings into account one can design effectively swimming nanorobots. In order to balance the torque produced on flagella, the body of the bacterium slowly rotate in opposite direction. Taking this into account and studying fluid dynamics may throw more light on this motion. The flexibility of flagellum also may play an important role in motion. Therefore including this in future studies will help us to understand more about this unique swimming mechanism.

References

[1] Lyttle A., Blanksby B. A., Elliot B. C., Lloyd D. G., 2000, "Net forces during tethered simulation of underwater streamlined gliding and kicking techniques of the freestyle turn," Journal of Sports Science, 18:801-807.

[2] Berg H. C., 1975, "Chemotaxis in bacteria," Annu Rev Biophys Bioeng., 4: 119–136.

[3] Silverman M., Simon M., 1974, "Flagellar Rotation and the Mechanism of Bacterial Motility," Nature 249:73-74.

[4] Namba K., 2004, February 5, "Revealing the mystery of the bacterial flagellum: A self-assembling nanomachine with fine switching capability (K Ishiguro, Interviewer)," Japan Nanonet Bulletin, No. 11 .

[5] Sivakumar M., Philominathan P., 2010, "The Physics of flagellar motion," Biophys Rev., 2:13–20.

[6] Sakar M. S., Lee1 C., and Arratia P. E., 2009, "Flagellar dynamics in viscous fluids," Phys. Fluids 21, 091107

[7] Flow Simulation 2010 Technical Reference, DSS.

[8] Hackbusch W., 1985, "Multi-grid Methods and Applications," NY, USA: Springer-Verlag.

[9] Hauke G., 2008, "An Introduction to Fluid Mechanics and Transport Phenomena," Dordrecht -Netherlands: Springer.

[10] Chattopadhyay S., Moldovan R., Chuck Y., Wu X. L., 2006, "Swimming efficiency of bacterium Escherichia coli," PNAS , 103:13712.